Contents

Chapter 1 3

Preliminary investigation of position dependency of radial diffusivity in the cervical spinal cord

In this experiment we investigate whether Diffusion Tensor Imaging (DTI) derived parameters are sensitive to the presence of collateral fibres and can be related the axial position of the acquired slice in the spinal cord (SC).

As this was my first MRI experience, this project helped me to get familiar with the anatomy of the SC and get hands on experience with DTI and the associated challenges of DTI in the SC. Although the number of control subjects is very small, the experience made in the setup of this study have significantly helped the design of subsequent experiments and development of new methods (e.g. see next chapter).

1.1 Motivation

The majority of Diffusion Weighted Imaging (DWI) studies mainly focused on the longitudinal fibres of the SC and ~~only~~ little is known about the value of DTI for the assessment of the connective collateral fibres. These fibres rise at an angle with the white-matter longitudinal tracts and enter the SC gray matter. They interconnect with other areas of the SC through the central gray matter and form part of many functional connections within the SC (Carpenter, 1991). Recently Mamata et al. (2006) demonstrated that the second eigenvector is corresponding to sprouting collateral fibres. In this study we focus on DTI of the SC *in-vivo* in healthy volunteers with particular interest in the diffusivity changes caused by the presence of the collateral fibres. We aim to investigate whether these DTI parameters are specific to nerve roots anatomy and therefore have the potential to be used in spinal cord injury (SCI) to assess the integrity of the axonal connections.

1.2 Methods

Our primary focus in this study was to develop a reliable and reproducible DTI pipeline incorporating acquisition, post-processing and analysis steps. In the following we explore several factors, such as slice positioning, number of signal averages, partial volume effect, that potentially have an effect on the outcome of the DTI analysis.

Positioning of DTI scans

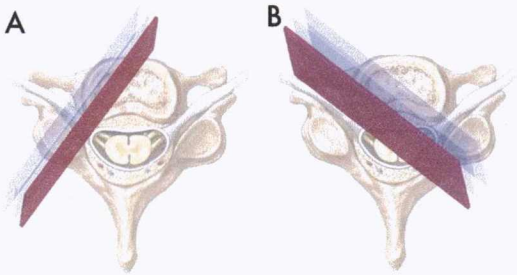

Figure 1.1: Illustration of the positions of the two sagittal oblique scans. The red colored slices illustrate the ideal positioning of the oblique scans. (A) The position of the first sagittal scan is intersecting the neuroforamen, (B) The second scan is aligned parallel to the spinal nerve root.

Accuracy and reproducibility in slice positioning for the DW acquisitions is crucial to discriminate differences in diffusion parameters between subjects. Since for this study we wanted to position our slices with respect to the neural foramina, a good visualization of the spinal nerve root is needed. However, finding the exact position of the nerve root is difficult on conventional axial or sagittal MRI scans. We use two sagittal oblique MRI scans to accurately reveal the location of the neuroforamen, similar to Goodman et al. (2006). Based on a standard axial scan of the cervical SC, we prescribed a sagittal scan that is approximately parallel to the spinal nerve leaving the neuroforamen (see Figure 1.1A). To visualize the SC and spinal nerve root a second sagittal oblique scan perpendicular to the first one is acquired. This scan is aligned so that at least one slice is parallel to the nerve root (see Figure 1.1B).

The first oblique scan is then used to position axial scans so that one slice intersects the spinal nerve. Figure 1.2 presents two scans acquired with this positioning. In Figure 1.2A one can clearly appreciate the neuroforamina between C4 and C7. Furthermore, in Figure 1.2B the spinal nerve root leaving the SC can be seen. Based on these scans we are able to accurately position the DW scans with respect to the roots anatomy. We assume that the diffusion parameters differ mostly between P1 and P2, i.e. the positions shown in Figure 1.2C, where P1 coincides with the level of the spinal nerve root leaving the SC and P2 with the vertebral body.

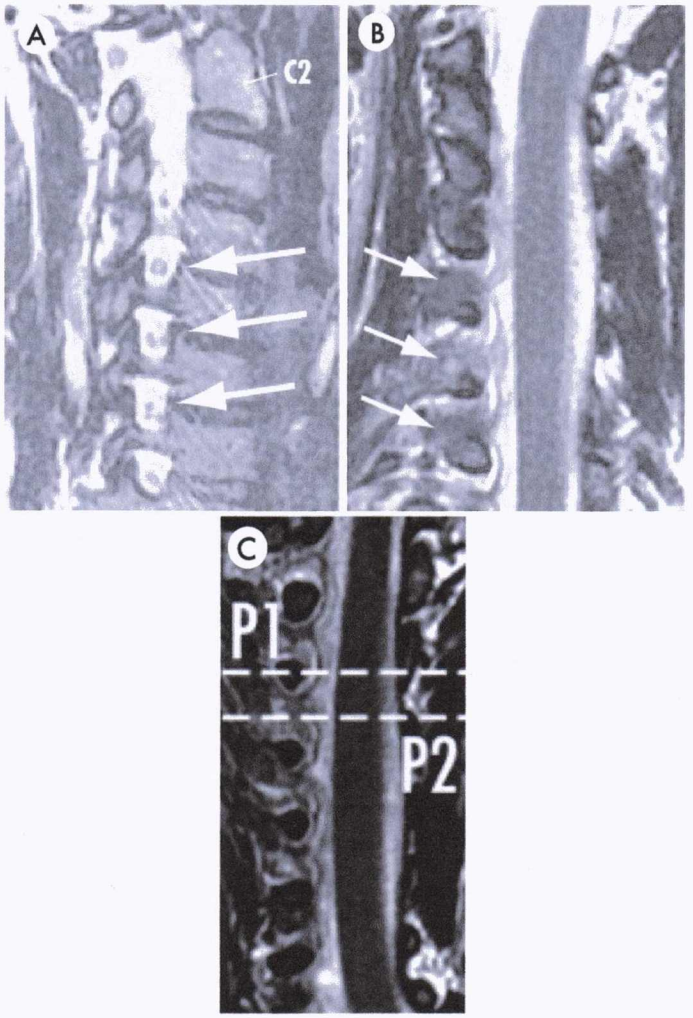

Figure 1.2: Example slices of the two sagittal oblique scans from one example subject. (A) The first sagittal oblique scan showing the neuroforamina of C4-C7 (white arrows). (B) The second oblique scan visualizing the spinal nerve roots (white arrows) (C) Positioning of the two DW axial scans based on the location of the spinal nerve roots.

Data acquisition

Diffusion-weighted scans are acquired on a 1.5T Signa scanner (General Electric Company, Milwaukee, WIS) using a four-channel phased-array spine coil. A cardiac-gated single shot CO-ZOOM EPI sequence (Dowell et al., 2009) was set up with the following imaging parameters: repetition time (TR) = 5RRs, echo time (TE)= 95.5ms, voxel size = $1 \times 1 \times 5mm^3$and an image matrix of 64×64 (field-of-view (FOV)=$13 \times 13mm^2$). After acquisition, all magnitude images are linearly interpolated to a 128×128 matrix on a slice-by-slice basis resulting in an in-plane resolution of 0.5x0.5 mm^2.

We acquire 8 distributed diffusion weighted directions (see Table 1.1) interleaved with 4 non-diffusion weighted directions. A b-factor of 1000 $s \cdot mm^{-2}$ was chosen for optimal Diffusion Tensor (DT)reconstruction as recommended in Jones & Basser (2004) for white matter fibres. We focus attention on a single slice acquisition to make sure that the signal from the slice is completely recovered after each shot, given that when using the CO-ZOOM sequence T1 relaxation can affect the signal intensity of subsequent slices in multiple slices acquisition. Also, by positioning one single slice, it is possible to acquire a SC image orthogonally to the main SC fibre direction. To increase signal-to-noise ratio we initially repeat each scan on each subject 22 times to determine the optimal number of averages needed. Subsequent scans on the same subject are repeated 15 times (see next section).

Data analysis

Table 1.1: Gradient directions for DTI acquisition. Lines marked with $*$ are used for $ADC_\perp$ reconstruction.

g_x	g_y	g_z
0	0	0*
0	0	0*
1	1	0*
0	1	1
1	0	1
0	0	0*
-1	-1	0*
0	1	-1
1	-1	0*
-1	0	1
-1	1	0*
0	0	0*

Registration Due to the relatively long scan time (30-40 minutes for 15 signal averages) the subject's position in the scanner is very likely to be affected by motion during the scan. However, registration of SC diffusion data is challenging for several reasons. First of all, diffusion-weighted images typically suffer from low SNR and low tissue contrast especially in the SC. Furthermore, in contrast to the brain, distortion artifacts from surround tissue and breathing motion make it difficult to identify reliable anatomical landmarks in the b=0 images. Moreover, longitudinal symmetry of the SC makes it impossible to correct for motion in this direction. Because of all these confounding factors, we use a restrictive motion model that only corrects for in-plane translation and assumes no movement in the z-direction. We divide data acquired within and between repetitions in different blocks with respect to the interleaved b=0 acquisitions. Each block starts with one b=0 image and contains all DW images up to the next b=0 acquisition. We then co-register two subsequent b=0 images using the VTK CISG registration toolkit (Hartkens et al., 2002). The resulting transformation is then applied to all the images of

one block. After registration, we average all scans with corresponding diffusion weighting from subsequent repetitions and all the b=0 acquisitions individually and perform the diffusion parameter estimation on the averaged data set as described below.

DTI analysis DT reconstruction is performed using the camino toolbox (Cook et al., 2006) and maps of the fractional anisotropy (FA) and radial diffusivity (RD) are calculated from the diffusion tensor (see section **??**). In addition we use an alternative method of measuring diffusivity in the axial plane ($ADC_{\perp}$) from only the 4 co-planar acquisitions with diffusion gradients perpendicular to the SC as described by Fasano et al. (2009). The used diffusion directions are marked "*" in Table 1.1). All calculations are implemented in MATLAB (Mathworks, Natick, MA). We include the $ADC_{\perp}$ method as it requires no measurements parallel to the fibre. Therefore the number of scans needed for reliable measurements is significantly reduced compared to a DTI acquisition, which can be extremely beneficial for future studies of SCI patients.

ROI analysis FA, RD and $ADC_{\perp}$ are quantified over the whole SC at each position. We semi-automatically segment the cord area on the average b=0 image of each slice using ImageJ[1] and the YAWI2D[2] segmentation plug-in. Due to the small size of the cord and the limits in image resolution, the segmented area will inevitably contain contributions from the surrounding cerebro-spinal fluid (CSF). Previous studies have shown that this partial volume considerably effects estimated diffusion parameters (Alexander et al., 2001; **?**). To minimize this effect, we applied a binary erosion filter on the resulting regions of interests. This removes pixels at the edge of the region of interest (ROI) and thus allows removing voxels with CSF contribution from the ROI analysis. Hereby the thickness of the removed edge is dependent on the size of the structure element that is used for the erosion filtering. Figure 1.3 illustrates the effect of the size of the structure element on the estimated diffusion parameters in one subject. It can be seen that in the initial segmentation, FA is underestimated and diffusivity measurements are overestimated respectively because of the isotropic free diffusion that is present in the voxels with CSF contribution. A structure element of size 2 proves to be sufficient to eliminate the partial volume effect and all measurements reach a stable plateau.

Signal averaging It is well known that in the low SNR regime the diffusion indices are very prone to estimation errors as shown in Pierpaoli & Basser (1996); Jones (2004); Landman et al. (2008). Thus, for reproducible measurements we need to acquire a sufficient number of averages in each scan. To determine the optimal number of averages for each subject we repeat the diffusion measurements at both slice positions 22 times each (overall scan time was approx. 1h). We then calculate the diffusion indices described above using a subset of the first N repeated measurements with N increasing from 1 to 22. A plot of mean diffusion indices over the SC against the number of averages is presented in Figure 1.4 for one representative subject. A significant bias can be observed in all diffusion indices when less than 10 averages are used. In none of

[1] `www.imagej.com`
[2] `yawi3d.sourceforge.net`

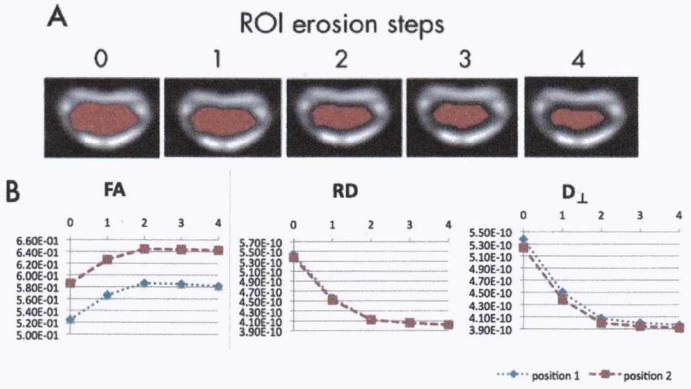

Figure 1.3: Effect of erosion of the ROI on measured parameters in one representative subject. (A) Illustration of the initial segmented ROI in one slice and the ROIs after erosion with structure elements of size 1-4. (B) Mean FA, RD and $ADC_{\perp}$ observed in the eroded ROIs.

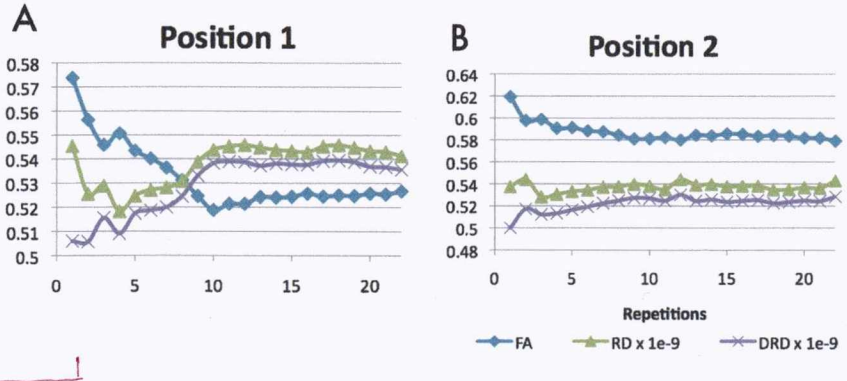

Figure 1.4: Plot of diffusion indices FA, RD and $ADC_{\perp}$ against number of averages. (A) shows the averaged diffusion parameter at nerve-root level (B) shows mean parameters at level of the body.

our subjects significant changes can be seen after 15 repetitions, so we choose the number of averages to be 15 in all subsequent scans.

Pilot study

A pilot study was carried out on 4 healthy female subjects. For each subject, parameter maps of FA, RD and $ADC_{\perp}$ were calculated as described above. We also calculated colour-coded maps of $\vec{v}_1, \vec{v}_2, \vec{v}_3$ for each scan. To assess intra-subject scan-rescan reproducibility, the scans were repeated with the same parameters after 5-7 days. Reproducibility of parameters was assessed by computing the coefficient of variation (COV) that is defined as the ratio of the standard deviation σ and the mean μ.

Table 1.2: COV of estimated parameters in all 4 subjects at both positions calculated from scan/re-scan experiment.

	FA		RD		$ADC_\perp$	
	P1	P2	P1	P2	P1	P2
Subject 1	0.3%	9.9%	3.6%	8.0%	5.2%	8.5%
Subject 2	11.9%	1.0%	6.6%	4.2%	7.7%	3.6%
Subject 3	3.8%	2.9%	2.9%	5.7%	3.8%	3.3%
Subject 4	4.7%	8.1%	1.2%	3.4%	2.4%	2.4%

1.3 Results and Discussion

Scan/rescan reproducibility

Table 1.2 shows the COV of all measured parameters in all four subjects. It can be seen that our careful approach towards positioning and analyzing the data allows good reproducibility (CoV $< 10\%$ in all but one cases) in the scan/rescan experiment among all subjects. Furthermore, it can be noted that parameter variation seems to be slightly elevated in the $ADC_\perp$ parameter compared to RD.

Single subject position dependency of measured parameters

Figure 1.5 compares the measured diffusion parameters between the two investigated positions in all subjects. FA and RD/$ADC_\perp$ are closely dependent, i.e. when FA is low RD and $ADC_\perp$ values are high and increasing FA corresponds to lower RD and $ADC_\perp$ in both positions. This implies that parallel diffusivity in the nerve fibres is position independent and therefore changes of FA between SC levels can be explained by different diffusivities perpendicular to the SC axis. Furthermore, it can be seen that the two methods of measuring diffusivity cross-sectionally give similar values in all subjects apart from minor differences in their standard deviation through the entire section of the cord. This can be explained by the lower number of only 4 diffusion measurements that are used to reconstruct $ADC_\perp$, compared to the 8 diffusion directions used for full DT reconstruction.

Between subjects comparision of position dependency of parameters

Although in individual subjects we can see differences between position 1 and 2 with little variation in parameters between scan and rescan, we find that these trends are not consistent between subjects. In subject 1 and subject 3 we observe lower RD/$ADC_\perp$ and higher FA at nerve root level compared to the vertebral body (see Figure 1.5). Subject 2 shows an opposite trend with higher FA at spinal root level and lower RD/$ADC_\perp$ respectively. In subject 4 there appear to be no differences between the two positions. It is unclear whether these differences between subjects can simply be explained by normal variation due to physiological noise or if they can be attributed to different fibre

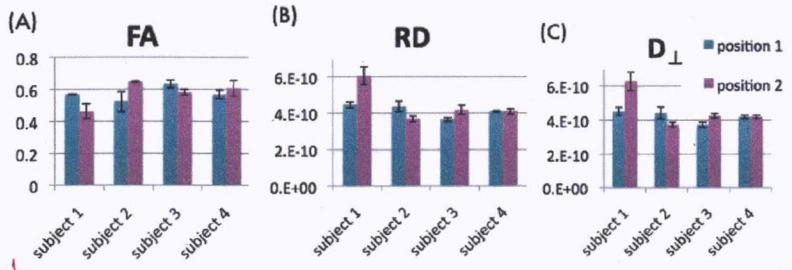

Figure 1.5: Measurements of FA, RD and $ADC_{\perp}$. Blue bars represent mean of measurements at nerve root level, red represent the mean of measurements at mid-vertebra level. Black error bars display the standard deviation between scan and rescan.

architecture in each individual. However, these differences between subjects also become apparent in the direction of the second eigenvector. In fact, it has been shown by Mamata et al. (2006) that the second DT eigenvector is sensitive to the presence of sprouting fibres in the SC. Figure 1.6 presents the color-coded maps of $\vec{v_2}$ overlaid on the FA map for two subjects with differing trends in diffusion parameters. Figure 1.6A displays $\vec{v_2}$ of subject 2, Figure 1.6B presents the $\vec{v_2}$-map of subject 4. In both cases, the first row shows the result from the first scan while the second row shows maps derived from the re-scan. The position of the slice in the second row (i.e. for the rescan) was chosen to correspond anatomically with the position of the slice in the first experiment presented in the first row. This was achieved using our 45° localization scanning method presented above and using a printout of the first scan positioning as reference. It has to be noted that a higher angular in-plane resolution of the diffusion gradient scheme would be needed to allow mapping real anatomical directions of the sprouting peripheral nerves. This however, would increase the number of acquisitions needed and therefore further increase the scan time. Moreover, even with our low-resolution scheme, distinct patterns emerge in each subject in the directions of the second eigenvector and are consistent over the first and second scan. Furthermore, in subject 2, where lower FA and higher $RD/ADC_{\perp}$ are present at spinal root level compared to mid-vertebra level, we also observe different patterns in position 1 and position 2. In subject 4, which shows no difference in mean diffusion parameters in P1 and P2, the $\vec{v_2}$ map is also similar in both positions. The same geometry is apparent in the repeated scans for both subjects.

These preliminary findings suggest that the diffusion measurements in the SC depend indeed on the presence of sprouting fibres. However, the organization of those fibres seems to be varying between subjects and needs to be addressed. The consistency of the patterns at different slice positioning between scans within each subject is encouraging because it suggests that DT parameters, and in particular $RD/ADC_{\perp}$, can be used in longitudinal studies to assess structural changes due to degeneration or regeneration of fibers. Table 1.2 shows the COV of all measured parameters in all four subjects. It can be seen that our careful approach towards positioning and analyzing the data allows good reproducibility (COV < 10% in all but one cases) in the scan/rescan experiment

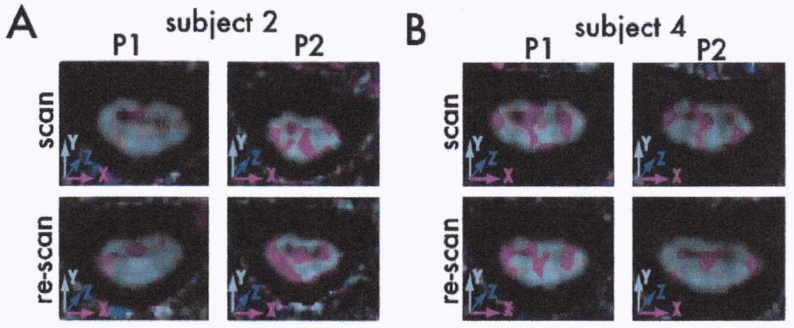

Figure 1.6: Color coded second eigenvector from DT overlaid on FA for two subjects. First row shows the first scan, second row the re-scan of two subjects. First column shows values at spinal root level, second column shows mid-vertebra position.

among all subjects.

1.4 Conclusion

This study investigated the position dependency of diffusion parameters measured in the cervical SC at two distinct levels. We concentrated on optimizing the acquisition protocol and the analysis procedure to eliminate the various confounding effects, e.g. from uncertainty in slice positioning, presence of physiological noise and subject motion as well as parameter estimation errors from partial volume effect. Furthermore, we were able to find differences between the two investigated positions consistently reproduced within subjects. Studies using $RD/ADC_{\perp}$ measurements in the SC will have to take into consideration the inter-subject variability of these parameters.

Related poster presentations

- Schneider, T., Alexander, D. C., & Wheeler-Kingshott, C. A. M. (2009). Preliminary Investigation of Position Dependency of Radial Diffusivity in the Cervical Spinal Cord. *17th Scientific Meeting of the International Society for Magnetic Resonance in Medicine*
- Schneider, T., Alexander, D. C., & Wheeler-Kingshott, C. A. M. (2009). Preliminary Investigation of Position Dependency of Radial Diffusivity in the Cervical Spinal Cord. *18th British Chapter ISMRM Postgraduate Symposium*

Bibliography

Alexander, A. L., Hasan, K. M., Lazar, M., Tsuruda, J. S., & Parker, D. L. (2001). Analysis of partial volume effects in diffusion-tensor {MRI}. *Magn Reson Med*, *45*(5), 770–780.

Carpenter, M. B. (1991). *Core Text of Neuroanatomy*. Lippincott Williams and Wilkins.

Cook, P., Bai, Y., Nedjati-Gilani, S., Seunarine, K., Hall, M. G., Parker, G. J. M., & Alexander, D. C. (2006). Camino: open-source diffusion-{MRI} reconstruction and processing. In *Proceedings 14th Scientific Meeting, International Society for Magnetic Resonance in Medicine*, (p. 2759).

Dowell, N. G., Jenkins, T. M., Ciccarelli, O., Miller, D. H., & Wheeler-Kingshott, C. A. M. (2009). Contiguous-slice zonally oblique multislice ({CO}-{ZOOM}) diffusion tensor imaging: examples of in vivo spinal cord and optic nerve applications. *J Magn Reson Imaging*, *29*(2), 454–460.

Fasano, F., Bozzali, M., Cercignani, M., & Hagberg, G. E. (2009). A highly sensitive radial diffusion measurement method for white matter tract investigation. *Magn Reson Imaging*, *27*(4), 519–530.

Goodman, B. S., Geffen, J. F., Mallempati, S., & Noble, B. R. (2006). {MRI} images at a 45-degree angle through the cervical neural foramina: a technique for improved visualization. *Pain Physician*, *9*(4), 327–332.

Hartkens, T., Rueckert, D., Schnabel, J., Hawkes, D., & Hill, D. (2002). {VTK} {CISG} Registration Toolkit. *BVM 2002*, (p. 409).

Jones, D. K. (2004). The effect of gradient sampling schemes on measures derived from diffusion tensor {MRI}: a Monte Carlo study. *Magn Reson Med*, *51*(4), 807–815.

Jones, D. K., & Basser, P. J. (2004). "Squashing peanuts and smashing pumpkins": how noise distorts diffusion-weighted {MR} data. *Magn Reson Med*, *52*(5), 979–993.

Landman, B. A., Farrell, J. A. D., Huang, H., Prince, J. L., & Mori, S. (2008). Diffusion Tensor Imaging at Low {SNR}: Non-monotonic behaviors of tensor contrasts. *Magn Reson Imaging*, *26*(6), 790.

Mamata, H., De Girolami, U., Hoge, W. S., Jolesz, F. A., & Maier, S. E. (2006). Collateral nerve fibers in human spinal cord: Visualization with magnetic resonance diffusion tensor imaging. *Neuroimage*, *31*(1), 24–30.

Missing 'J'?

Pierpaoli, C., & Basser, P. J. (1996). Toward a quantitative assessment of diffusion anisotropy. *Magn Reson Med*, *36*(6), 893–906.